Research in Veterinary Science 140 (2021) 134–141

Contents lists available at ScienceDirect

Research in Veterinary Science

journal homepage: www.elsevier.com/locate/rvsc

Proteomic analysis of the secretome of equine herpesvirus-1 infected rabbit kidney cells

Wojciech Rozek [a,*], Malgorzata Kwasnik [a], Agata Malinowska [b], Karol Stasiak [a], Magdalena Larska [a], Jerzy Rola [a]

[a] Department of Virology, National Veterinary Research Institute, 24-100 Pulawy, Poland
[b] Environmental Laboratory of Mass Spectrometry, Polish Academy of Sciences, Institute of Biochemistry and Biophysics, 02-106 Warsaw, Poland

ARTICLE INFO

Keywords:
Equine herpesvirus
EHV-1
UPR
Calreticulin
Endoplasmin
Hspa5

ABSTRACT

Herpesviruses are the main cause of abortions and respiratory or neurological disorders in horses. Various disease patterns are suspected to be associated with the A2254G point mutation in the DNA polymerase sequence (ORF30) of the herpesvirus genome, although the importance of this link is still under debate. Based on a label-free quantitative proteomic analysis, the differences in the secretion of some host proteins between rabbit kidney cells infected with A_{2254} and cells of the same line infected with G_{2254} equine herpesvirus 1 (EHV-1) strains were identified. In both groups, downregulation of proteins involved in insulin growth factor and extracellular matrix pathway regulation was observed. Among 12 proteins with increased secretion, 8 were regulated only in G_{2254} EHV-1 infection. Those were endoplasmic reticulum chaperones with calcium binding properties, related to unfolded protein response and mitochondria. It was presumed that the secretion of proteins such as calreticulin, Hspa5 or endoplasmin may contribute to the pathogenesis of EHV-1 infection.

1. Introduction

Equine herpesvirus-1 (EHV-1) is a pathogen causing abortion, respiratory disease and neurological disorders in horses worldwide (Kydd et al., 2019). Although most EHV-1 strains can induce abortion, only specific strains have the potential to cause equine herpesvirus myeloencephalopathy (EHM) (Oladunni et al., 2019). Endothelial cell invasion and inflammation of the vasculature of the CNS are the key features of this neurological syndrome (Edington et al., 1986; Holz et al., 2019). Nugent et al. (2006) proposed the link between a point mutation in the virus' DNA polymerase ORF 30 (A2254G, N752D) and increased frequency of neurological disease. However, factors other than the point mutation are likely to be associated with neurological symptoms (Pronost et al., 2010). In the mechanism of EHV-1 neuropathogenesis the role of viral DNA polymerase, glycoprotein D, interferons, interleukins, and chemokines CXCL9 and CXCL10 has been postulated (Holz et al., 2017; Poelaert et al., 2019, 2018). It was also confirmed that the G_{2254} EHV-1 strains replicate more efficiently in horses and produce a higher virus titer than A_{2254} strains (Allen and Breathnach, 2006). Both virus strains replicated with similar kinetics in fibroblasts and epithelial cells, but showed differences in leukocyte tropism. A significant increase was observed in the sensitivity of A_{2254} EHV-1 to afidicoline, a drug acting on viral polymerase (Goodman et al., 2007). Additionally, it was shown that A_{2254} strains were more sensitive to acyclovir than G_{2254} strains, based on viremia measurements (Sutton et al., 2020). The above findings indicate the association of different biological properties of EHV-1 with the A2254G mutation.

Proteomic analysis of the secretome of infected cells may contribute to a better understanding of the pathogenesis of herpesvirus infection (Hensel et al., 2020). The aim of our study was to define the differences in the protein secretion between A_{2254} and G_{2254} EHV-1 infected cells. It should be noted that rabbit kidney cells were used in the experiment and the results obtained in this model may not fully reflect the virus–cell interaction during *in vivo* infection of horses.

2. Materials and methods

2.1. Viruses

Laboratory reference strains and domestic isolates of G_{2254} EHV-1 (Ab4, PL/2009/II and PL/2010/II) and A_{2254} EHV-1 (Kentucky D, 438/77 and PL/2016/II) were used (Stasiak et al., 2015). Viral strains

* Corresponding author at: National Veterinary Research Institute, Partyzantow 57, 24-100 Pulawy, Poland.
E-mail address: wojciech.rozek@piwet.pulawy.pl (W. Rozek).

https://doi.org/10.1016/j.rvsc.2021.08.014
Received 18 February 2021; Received in revised form 30 July 2021; Accepted 12 August 2021
Available online 17 August 2021
0034-5288/© 2021 The Authors. Published by Elsevier Ltd. This is an open access article under the CC BY-NC-ND license (http://creativecommons.org/licenses/by-nc-nd/4.0/).

Table 1
Differentially expressed proteins (DEPs) secreted in G_{2254} or A_{2254} EHV-1 strain infection.

NCBI ID	q-value	Fold change	Gene	Protein name	Morphological & functional annotation*				
					ER	MITO	UPR	IGF	ECM
Upregulated – G_{2254}:									
XP008256277.1	0.00455	1.49	Pdia4	protein disulfide-isomerase A4	v				
XP002711121.1	0.03313	1.48	Cs	citrate synthase, mitochondrial		v			
AAB20096.1	0.00708	1.46	Calr	calreticulin	v		v		
NP001075637.2	0.03422	1.43	YWHAQ	14-3-3 protein theta					
XP017205553.1	0.01151	1.36	Hspa5	78 kDa glucose-regulated protein	v		v		
XP002710287.1	0.03902	1.35	Hspa9	stress-70 protein, mitochondrial		v	v		
ABD77238.1	0.02965	1.34	ATP5B	mitochondrial ATP synthase		v			
XP008255217.1	0.01252	1.32	Hsp90b1	endoplasmin	v		v	v	
Downregulated – G_{2254}:									
XP017204105.1	0.02246	7.84	SEC23IP	SEC23-interacting protein	v				
XP002710791.1	0.02133	1.76	EXT1	exostosin-1	v				
XP008269665.1	0.04860	1.75	Serping1	plasma protease C1 inhibitor					
XP017201501.1	0.04434	1.74	Csf1	macrophage colony-stimulating factor 1	v			v	
XP017196042.1	0.03286	1.73	KLRK1	NKG2D ligand 2-like					
ABQ23981.1	0.02765	1.72	MAM	nephronectin					
XP017194041.1	0.04187	1.71	NEO1	neogenin					
XP008266038.1	0.00248	1.69	Igfbp7	IGF-binding protein 7	v			v	
XP002708816.2	0.00269	1.65	TPP1	tripeptidyl-peptidase 1					
XP008267279.1	0.01110	1.62	Fbn1	fibrillin-1	v			v	v
XP008269801.1	0.00591	1.61	GRN	granulins	v				
XP002721425.1	0.00284	1.60	NAGA	alpha-N-acetylgalactosaminidase					
XP002710192.1	0.00185	1.59	LOX	protein-lysine 6-oxidase isoform X2					v
XP008250585.1	0.00052	1.56	Nucb1	nucleobindin-1	v			v	
XP002719886.1	0.03319	1.53	ATP6AP2	renin receptor					
AAV34702.1	0.03638	1.51	HEXB	beta-hexosaminidase beta-subunit					
XP008268321.1	0.02120	1.51	EXT2	exostosin-2	v				
ABQ23962.1	0.00052	1.49	Ctsb	cathepsin B					v
XP002723857.2	0.04768	1.49	PXDN	peroxidasin homolog isoform X1	v				v
XP017200326.1	0.00433	1.49	CD109	CD109					
Q9TRZ7.1	0.03313	1.48	Timp2	Metalloproteinase inhibitor 2					v
NP001076175.1	0.00465	1.47	Cst3	cystatin-C	v			v	
XP008265088.1	0.00376	1.47	Fstl1	follistatin-related protein 1	v			v	
NP001164511.1	0.03293	1.46	MET	hepatocyte growth factor receptor					
XP002715057.1	0.00490	1.46	Qsox1	sulfhydryl oxidase 1	v			v	
XP002723887.2	0.02839	1.45	Loxl1	lysyl oxidase homolog 1					v
XP002712513.1	0.00131	1.44	IGFBP2	IGF-binding protein 2				v	
XP008251825.1	0.00010	1.44	CTSD	cathepsin D					v
XP008267930.1	0.00213	1.39	CD44	CD44 antigen isoform X5					v
XP008250933.1	0.03079	1.38	RNASET2	ribonuclease T2	v				
XP008251456.2	0.03158	1.38	COL18A1	collagen alpha-1(XVIII) chain	v				v
Upregulated – A_{2254}:									
XP002711597.1	0.00609	1.43	GOT2	aspartate aminotransferase, mitochondrial		v			
XP008257460.1	0.04358	1.33	SERPINE2	glia-derived nexin					
Downregulated – A_{2254}:									
NP001075488.1	0.00822	1.56	ANXA8	annexin A8					
XP017194515.1	0.01324	1.43	TLN1	talin-1 isoform X4					

* Morphological and functional annotations based on STRING analysis: ER – GO:0005783 "Cellular Component – endoplasmic reticulum", MITO – GO:0005759 "Cellular Component – mitochondrial matrix", UPR – GO:0051082 "Molecular Function – unfolded protein binding", IGF – HSA-381426 "Reactome Pathways – Regulation of Insulin-like Growth Factor (IGF) transport and uptake by Insulin-like Growth Factor Binding Proteins (IGFBPs)", ECM – R-HSA-1474244 "Reactome Pathways – Extracellular matrix (ECM) organization".

were propagated and titrated in rabbit kidney 13 (RK13) cells (CCL-37™, ATCC®).

2.2. Virus infection studies and sample preparation

Cells were cultured in Eagle's medium supplemented with 10% fetal bovine serum in 75 cm^2 flasks. They were washed twice with PBS and the virus was applied at MOI 0.5. After 1 h adsorption, the RK13 cells were washed and maintained in serum-free medium. Mock-infected cells were used as a control. After 24 h post infection (hpi), culture fluids were collected. A cytotoxicity assay (Lactate Dehydrogenase (LDH) Kit, Roche, Mannheim, Germany) was performed according to the manufacturer's recommended procedure. For proteomic analysis culture fluids were centrifuged at 600 ×*g* for 10 min at 4 °C and then at 100000 × g for 2 h at 4 °C with a type 45 Ti rotor (Beckman-Coulter, Indianapolis, IN, USA). The supernatants were concentrated on 3 kDa cut-off filters (UFC900324, Merck KGaA, Darmstadt, Germany). Proteins were precipitated with acetone (−20 °C), the pellets were suspended in 100 mM ammonium bicarbonate, and the proteins were reduced using 0.5 M TCEP for 1 h at 57 °C and alkylated with 200 mM MMTS for 10 min in the dark. The proteins were subsequently digested overnight with trypsin (V5111, Promega, 0.01 μg per 1 μg of protein) and the reaction was quenched with 0.1% TCA.

2.3. Label-free protein quantification and data analysis

Mass spectrometry label-free quantification was performed as previously described (Malinowska et al., 2012). Samples were measured using a Q Exactive spectrometer (ThermoFisher Scientific, Waltham, MA, USA) coupled with a nanoACQUITY UPLC system (Waters Corporation, Milford, MA, USA). Proteins were identified with Mascot Server 2.5 using databases of virus (NCBInr 20,180,903 and 2,311,225) and rabbit (NCBInr 20,180,903 and 37,910) amino acid sequences and verified with the target-decoy strategy. Data analysis was performed

Table 2
Differentially expressed proteins (DEPs) secreted during infection with both G_{2254} and A_{2254} EHV-1 stains.

NCBI ID	q-value	Fold change	Gene	Protein name	Morphological & functional annotation*				
					ER	MITO	UPR	IGF	ECM
Upregulated - both groups G_{2254} and A_{2254}:									
XP002712414.1	0.00142	1.37	HSPD1	60 kDa heat shock protein, mitochondrial		v	v		
	0.00873	1.41							
NP001075526.1	0.00010	1.31	PPIA	peptidyl-prolyl cis-trans isomerase A			v		
	0.00028	1.38							
Downregulated - both groups G_{2254} and A_{2254}:									
P017205630.1	0.00010	1.94	FSTL5	follistatin-related protein 5 isoform X1					
	0.00310	1.64							
P98118.1	0.00010	1.87	PROS1	Vitamin K-dependent protein S	v				
	0.00627	1.57							
XP002719754.1	0.00010	1.9	TCN2	transcobalamin-2					
	0.00192	1.5							
ACJ73996.1	0.00324	1.49	CDH2	cadherin 2	v			v	
	0.04976	1.32							
NP001095170.1	0.00010	1.52	DAG1	dystroglycan precursor	v				v
	0.00016	1.40							
NP001076101.1	0.00010	1.78	SOD3	extracellular superoxide dismutase					
	0.00312	1.46							
XP008248493.1	0.00250	1.42	BGN	biglycan isoform X1					v
	0.00016	1.61							
XP008272128.1	0.00010	1.63	CLU	clusterin isoform X1	v				
	0.00016	1.60							
XP017200867.1	0.00010	1.86	CTGF	connective tissue growth factor					
	0.00016	1.36							
XP002724384.1	0.00010	1.52	LGALS3BP	galectin-3-binding protein					
	0.00016	1.65							
XP008248965.2	0.00034	1.45	ICAM1	intercellular adhesion mol.1 isoform X1					v
	0.00370	1.36							
XP002714822.1	0.00914	1.52	FUCA2	plasma alpha-L-fucosidase	v			v	
	0.04831	1.36							
XP002714872.1	0.00266	1.51	VNN3	vascular non-inflammatory molecule 3					
	0.00016	1.53							
AAW79053.1	0.00421	1.59	TIMP-1	tissue inhibitor of metalloproteinase 1	v			v	v
	0.04958	1.52							

* Morphological and functional annotations based on STRING analysis: ER – GO:0005783 "Cellular Component – endoplasmic reticulum", MITO – GO:0005759 "Cellular Component – mitochondrial matrix", UPR – GO:0051082 "Molecular Function – unfolded protein binding", IGF – HSA-381426 "Reactome Pathways – Regulation of Insulin-like Growth Factor (IGF) transport and uptake by Insulin-like Growth Factor Binding Proteins (IGFBPs)", ECM – R-HSA-1474244 "Reactome Pathways – Extracellular matrix (ECM) organization".

with in-house developed MScan and Diffprot software (Malinowska et al., 2012). The SecretomeP algorithm was used to predict non-classical protein secretion or the presence of the signal peptide (Bendtsen et al., 2004) and protein interaction network analysis was performed using the STRING Pathways database (v11.0) (Szklarczyk et al., 2015).

2.4. Immunoblotting

Immunoblotting was carried out as described previously (Rozek et al., 2013). Twenty micrograms of protein was loaded and reacted with antibodies against calreticulin (ab4109, Abcam, Cambridge, UK), heat shock protein family A member 5 (Hspa5) (ABIN863113, Antibodies-online, Aachen, Germany) or endoplasmin (ab233979, Abcam, Cambridge, UK). A total protein staining was performed using Sypro™ Ruby (Invitrogen, Waltham, MA, USA) according to the manufacturer's procedure. The chemiluminescence and fluorescence signals were captured and analyzed using an LAS3000 luminescent image analyzer (FujiFilm Life Sciences, Stanford, CT, USA). The signal ratios of proteins secreted during EHV-1 infection to those of uninfected cells were determined for calreticulin, Hspa5 and endoplasmin.

2.5. Statistical analysis

Non parametric statistical analysis of MS–derived data for differential proteomic was performed using Diffprot – software (Malinowska et al., 2012). Diffprot was run with the following parameters: number of random peptide sets = 10^6, clustering of peptide sets—only when 90% identical. Prior to analysis, quantitative values were normalized with LOWESS. Data were considered statistically significant when $q < 0.05$. Immunoblot signal intensities were normalized based on total protein staining according to Aldridge et al. (2008). Statistical significance for both immunoblot and LDH analyses was determined using *t*-test.

3. Results

A total of 1201 proteins were identified in the secretome of uninfected RK13 cells and of those infected with EHV-1 (at least 2 peptides per protein, FDR < 1%). The number of proteins detected in experimental groups ranged between 597 and 847 (804–847 for G_{2254} strains, 775–847 for A_{2254} strains and 597–786 for uninfected cells). The mass spectrometry proteomics data have been deposited with the ProteomeXchange Consortium/PRIDE (Perez-Riverol et al., 2019) under number PXD017534.

Label-free quantitative proteomic analysis was carried out by the comparison of peptides derived from proteins secreted from cells infected with G_{2254} or A_{2254} EHV-1 with those secreted by uninfected control cells. Analysis revealed statistically significant ($q < 0.05$) differential expression of 59 proteins (fold change, FC > 1.3). Among them, 39 were regulated only in G_{2254} EHV-1 infection (8 up- and 31 downregulated), 4 were in A_{2254} EHV-1 infection (2 up- and 2 downregulated) (Table 1) and 16 in both cases (2 up- and 14 downregulated) (Table 2).

STRING, protein–protein interaction network analysis showed the clustering of 55 out of 59 differentially expressed proteins. They were annotated to different morphological and functional categories, with the most pronounced being GO:0005783 "Cellular Component –

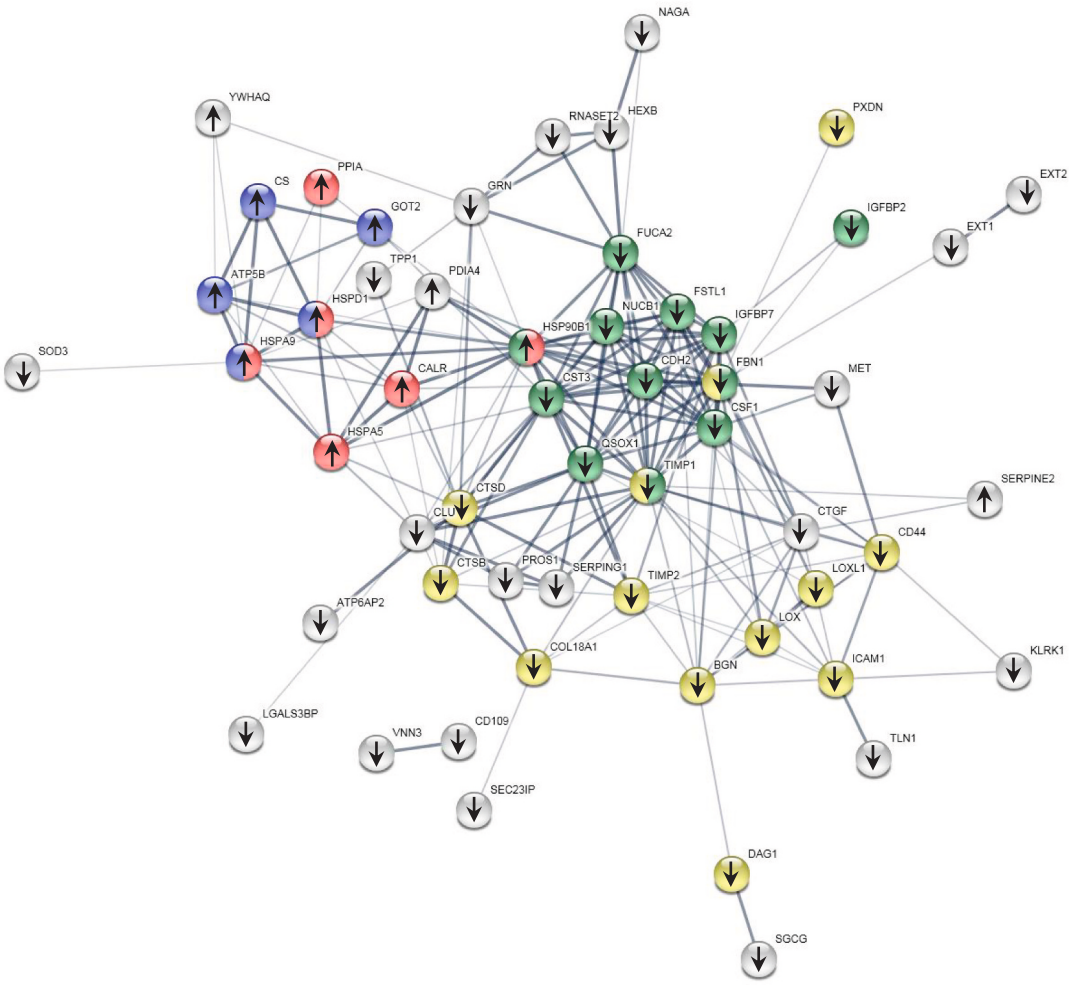

Fig. 1. The interaction network of proteins altered in the secretome of EHV-1 infected cells, STRING pathways analysis. Arrows indicate up- and downregulation, colors indicate GO annotations: red – GO: 0051082 "Molecular Function – unfolded protein binding"; blue – GO:0005759 "Cellular Component – mitochondrial matrix"; green – HSA-381426 "Reactome Pathways – Regulation of Insulin-like Growth Factor (IGF) transport and uptake by Insulin-like Growth Factor Binding Proteins (IGFBPs)"; yellow – R-HSA-1474244 "Reactome Pathways – Extracellular matrix organization". (For interpretation of the references to colour in this figure legend, the reader is referred to the web version of this article.)

endoplasmic reticulum" (24 proteins, FDR = 1.91e−09), GO:0005759 "Cellular Component – mitochondrial matrix" (5 proteins, FDR = 0.0439), GO:0051082 "Molecular Function – unfolded protein binding" (6 proteins, FDR = 0.00028), HSA-381426 "Reactome Pathways – regulation of insulin-like growth factor (IGF) transport and uptake by insulin-like growth factor binding proteins (IGFBPs)" (12 proteins, FDR = 1.45e−12), and R-HSA-1474244 "Reactome Pathways – extracellular matrix (ECM) organization" (13 proteins, FDR = 5.43e−10) (Fig. 1, Tables 1 and 2). Functional categories of proteins were clearly distinguished in terms of their up- or downregulation in the secretome of EHV-1 infected cells. Unfolded protein binding group and mitochondrial matrix proteins were upregulated, while proteins involved in the IGF and ECM pathways were downregulated (except for endoplasmin assigned to both the unfolded protein response (UPR) and IGF pathways). Some of these proteins were regulated only during infection with G_{2254} strains (Table 1, Fig. 2A). SecretomeP analysis showed the predicted signal peptide for 30 out of 59 proteins, and another 9 proteins showed a neural network (NN) score above 0.6 and were classified as potentially secreted by the non-classical pathway (Supplementary Table S1).

Three proteins upregulated in the secretome of G_{2254}-infected cells and related to UPR were analyzed by immunoblot. The analysis showed upregulation of calreticulin, endoplasmin and Hspa5 secreted by cells infected with G_{2254} EHV-1 relative to that secreted by cells infected with A_{2254} EHV-1 (Fig. 2B). The LDH release assay showed no significant differences in the cytotoxicities of A_{2254} and G_{2254} EHV-1 strains to RK13 cells (Fig. 3).

4. Discussion

Analysis of the protein composition of the secretome of virus-infected cells may reveal processes crucial for the pathogenesis of infection (Hensel et al., 2020). We identified secreted host proteins that were changed in abundance by EHV-1 infection. It can be assumed that the differences in biological properties of EHV-1 strains carrying the G_{2254} or A_{2254} mutation (*e.g.* potential neuropathogenicity) may be reflected in the variant secretomes of infected cells. In general, most of the differentially expressed proteins (DEPs) were downregulated (47 out of 59 proteins), of which a significant group were those classified as involved in the IGF and ECM pathways. Twelve proteins with increased secretion were identified. Among them, eight were upregulated only during G_{2254} EHV-1 infection: calreticulin, PDIA4, Hspa5, endoplasmin, 14–3-3 protein theta, citrate synthase, Hspa9 and ATP5B. Most of them act as ER chaperones, have calcium binding properties and are related to UPR (Halperin et al., 2014; Michalak et al., 2002).

The secretion of ER-luminal chaperones with Ca^{2+} binding

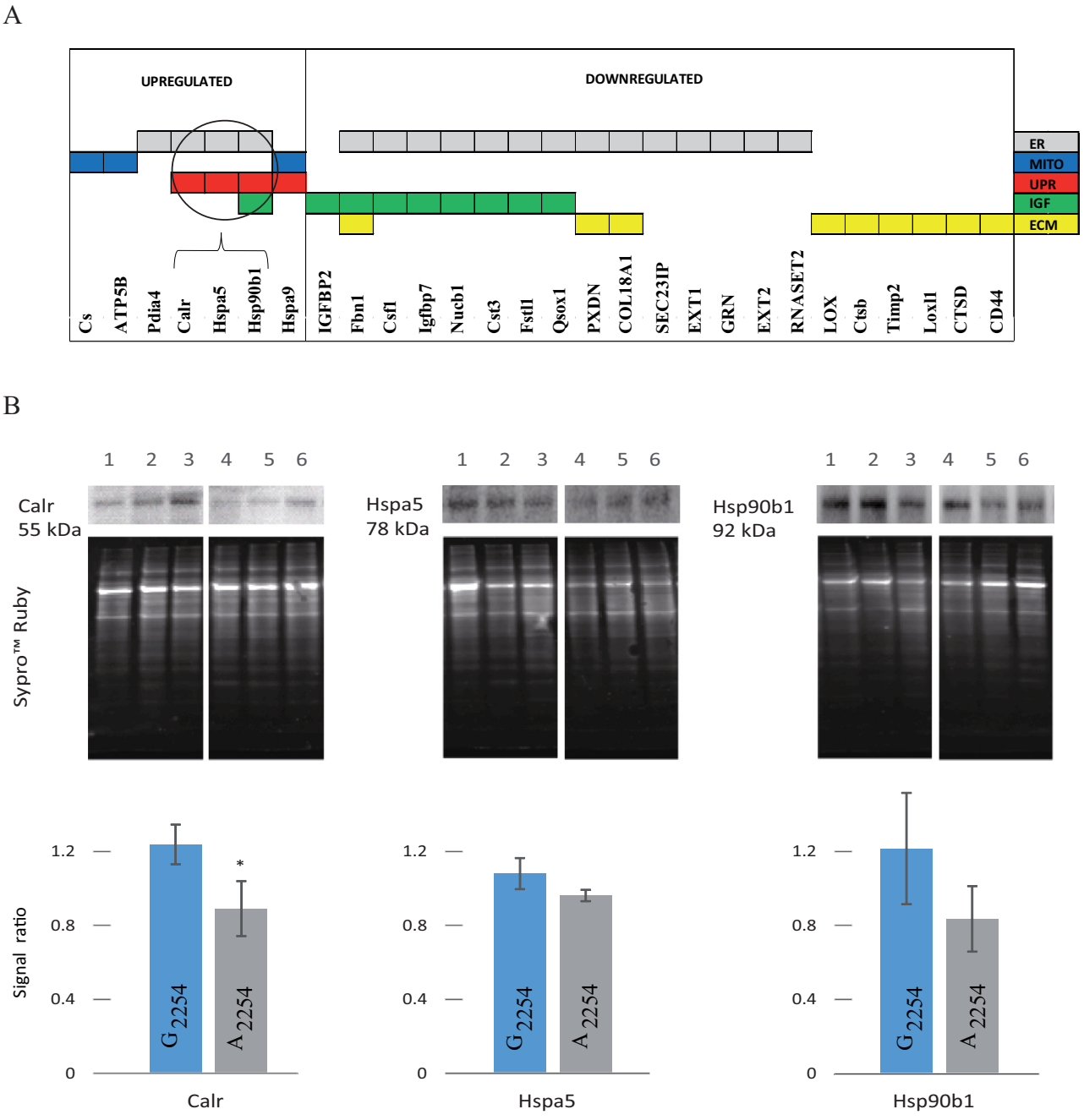

Fig. 2. A – Classification of the up- and downregulated proteins in the secretome of G_{2254} EHV-1-infected cells to morphological or functional categories: endoplasmic reticulum (ER), mitochondrion (MITO), unfolded protein response (UPR) pathway, insulin-like growth factor (IGF) and extracellular matrix (ECM) regulation; calreticulin (Calr), Hspa5 and endoplasmin (Hsp90b1) were indicated. B – Immunoblot analysis of Calr, Hspa5 and Hsp90b1 secreted by EHV-1-infected cells. Three G_{2254} (Ab4, PL/2009/II and PL/2010/II) (lines 1–3) and three A_{2254} (Kentucky D, 438/77 and PL/2016/II) (lines 4–6) EHV-1 strains were used. Signal intensity was normalized based on a total protein staining (Sypro™ Ruby). The column charts show the normalized signal intensity ratios of G_{2254} or A_{2254} EHV-1 to the uninfected control: blue – G_{2254} EHV-1; gray – A_{2254} EHV-1. Error bars represent ±1 SD signal ratio for triplicates (* – $p < 0.05$, $p = 0.027$ for Calr, $p = 0.067$ for Hspa5, $p = 0.065$ for Hsp90b1, *t*-test). (For interpretation of the references to colour in this figure legend, the reader is referred to the web version of this article.)

properties was investigated previously in the secretome of cardiac myocytes treated with thapsigargin (an ER stressor which depletes ER calcium), when increased secretion of Hspa5 (GRP78), endoplasmin (GRP94) and calreticulin was observed and was also caused by simulated ischemia (Blackwood et al., 2020). We observed increased secretion of the same set of proteins. Perhaps similar processes, accompanied by deregulation of calcium homeostasis, also take place during G_{2254} EHV-1 infection, although this would require further studies to confirm. Van Cleemput et al. (2017) analyzed access to the basolaterally located alphaherpesvirus receptor in equine respiratory cells. EHV1 infection of equine mucosal explants was greatly enhanced upon destruction of the respiratory epithelium integrity with EGTA or *N*-acetylcysteine, which are drugs affecting extra- and intracellular calcium levels. Restriction of infection *via* apical inoculation was overcome by disruption of intercellular junctions. The authors used explants, which perfectly mimics the situation *in vivo*. It cannot be ruled out that also the secretion of calcium binding proteins (*e.g.* calreticulin) may lead to loosening of the intercellular junctions (by capturing Ca^{2+}), facilitating access to

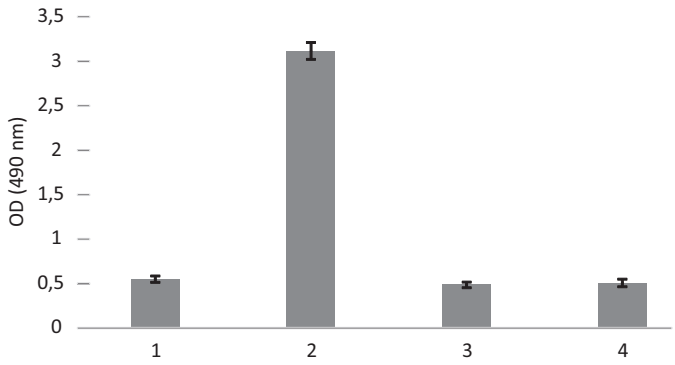

Fig. 3. Cytotoxicity assay – Lactate Dehydrogenase (LDH) for cell culture fluids of RK13 cells infected with EHV-1. 1 – uninfected RK13 cells, 2 – cells treated with Triton X-100 (positive control), 3 – cells infected with G_{2254} EHV-1 strains, 4 – cells infected with A_{2254} EHV-1 strains. Error bars represent ±1 SD of OD values. There were no statistically significant differences in cytotoxicity induced by G_{2254} and A_{2254} EHV-1 strains ($p > 0.19$, *t*-test).

basolaterally located viral receptors and in consequence also infection. The extracellular role of ER chaperones has been studied previously in various aspects (Meyer and Doroudgar, 2020). Extracellular endoplasmin has been seen to be involved in immunological responses, dendritic cell activation and spontaneous autoimmune diseases (Jockheck-Clark et al., 2010; Liu et al., 2003). The extracellular functions of calreticulin include cutaneous wound healing (Greives et al., 2012), induction of cancer cell death (Obeid et al., 2007) and promotion of phagocytosis of cancer and apoptotic cells (Gardai et al., 2005; Meyer and Doroudgar, 2020). Hspa5 (GRP78) was identified on the surface of endothelium and monocyte/macrophage-like cells in atherosclerotic lesions, and it was shown that this protein negatively regulates tissue factor procoagulant activity (Bhattacharjee et al., 2005). It can also act as a co-receptor for various viruses, notably Coxsackie A9 virus, dengue serotype 2 virus, Borna disease virus and Japanese encephalitis virus (Honda et al., 2009; Jindadamrongwech et al., 2004; Nain et al., 2017; Triantafilou et al., 2002). This protein is also involved in coronavirus attachment, as it has binding sites to viral spike proteins (Chu et al., 2018; Ibrahim et al., 2020). The question arises whether the extracellular activity of ER chaperones might contribute to EHV-1 neuropathogenesis. Following infection of the respiratory epithelium, EHV-1 crosses the basement membrane by the use of infected leukocytes, which penetrate the connective tissues and reach the bloodstream. They can adhere to and subsequently transfer EHV-1 to the endothelial cells lining the blood vessels of organs such as the pregnant uterus or CNS (Laval et al., 2021). The proteins we observed, secreted during G_{2254} or A_{2254} EHV-1 infection, could be involved as factors facilitating the infection of specific cells or target organs.

The accumulation of unfolded proteins can lead to proteostasis disorders inside the ER, and as a result UPR signaling is activated (Gardner et al., 2013). The activation of ER-resident stress sensors, activating transcription factor 6 (ATF6), phosphorylated extracellular signal-related kinase (PERK) and inositol-requiring transmembrane kinase/endoribonuclease 1α (IRE1α) affects molecular pathways related to increased protein folding capacity, secretion, quality control and protein degradation (Walter and Ron, 2011). Endoplasmic reticulum stress may induce cell death with broad consequences in different pathologies (neurological and cardiovascular diseases, ophthalmic disorders, viral infections and diabetes) (da Silva et al., 2020; Kaufman, 2002; Scheuner and Kaufman, 2008). It has been reported that infection with some neurotropic viruses (Zika, West Nile or human herpesvirus 1) can impact UPR (Alfano et al., 2019; Burnett et al., 2012; Medigeshi et al., 2007). It was found that the intensification of viral glycoprotein synthesis during lytic herpesvirus replication causes ER stress and these viruses may have evolved mechanisms to manage UPR signaling to create an optimal niche for replication (Johnston and McCormick, 2019). Increased secretion of UPR-related proteins by G_{2254} EHV-1 infected cells may be related to overexpression of these proteins or indicate the mechanism of UPR limitation, however these hypotheses need further investigation.

Among the proteins upregulated during G_{2254} infection were mitochondrial proteins. The ER and mitochondria are closely associated *via* specific membrane contact sites and create dynamic molecular platforms referred to as mitochondria-associated membranes (MAMs) (Giorgi et al., 2015). Calreticulin is one of the proteins associated with ER and MAMs. Dysfunctions of mitochondria and the ER-mitochondria crosstalk are linked to ageing and neurodegeneration (Barodia et al., 2019; Moltedo et al., 2019). Proteins found to be upregulated in the secretome of G_{2254} EHV-1-infected cells in our study (citrate synthase, Hspa9 and ATP5B) have been reported as associated with mitochondrial stress.

Downregulation of IGF binding proteins in the secretome of EHV-1 infected cells may be linked to the secretion of ER chaperones. Ostrovsky et al. (2009) reported that IGF-II secretion is strictly dependent on the ER chaperone endoplasmin (GRP94); in the absence of endoplasmin activity, IGF-II intermediates undergo proteasome-dependent degradation. Heat shock proteins and molecular chaperones are involved in the regulatory processes that determine the assembly and degradation of the ECM at multiple levels (Boel and Edkins, 2018). The lower level of proteins assigned to the extracellular matrix in the secretome of cells infected with G_{2254} EHV-1 (cathepsin B and Timp2) may also indicate the importance of proteolysis regulation in the pathogenesis of EHV-1 infection.

We used the SecretomeP algorithm to determine the secretory potential of the analyzed proteins. The signal peptide was predicted for 51% of the proteins. The presence of this peptide enables the functioning of the conventional protein secretion pathway, translocation into ER, and transport through the Golgi complex and secretory vesicles (Kelly, 1985). Additionally, 15% of the proteins, which had NN scores above 0.6, were predicted as potentially secreted through the unconventional secretory pathway (Supplementary Table S1). However, NN scores below 0.6 do not preclude proteins being secreted by other mechanisms. It is possible that during EHV-1 infection, dysregulation of protein secretion pathways occurs.

The RK13 cells were used in the study as they support infection by a variety of field EHV-1 viruses and comprise a homogeneous population of cells. The use of primary equine cells may have provided a better reflection of the virus-host interactions, but the virus-induced changes in the cell proteome may have been more difficult to decipher against the background of a heterogeneous population of primary cells. Irrespective of the cell system used, the results of any *in vitro* study, including this one, should be interpreted with caution and confirmed using *in vivo* experiments.

In conclusion, we identified proteins up- or downregulated in the secretome of equine herpesvirus infected cells, and compared the regulation of these proteins during G_{2254} and A_{2254} EHV-1 infection. Unfolded protein response–related ER chaperones secreted specifically for G_{2254} EHV-1 infection could potentially be important in neuropathogenesis. Considering that the genotype does not clearly determine the occurrence of EHM, these observations require further analysis and confirmation.

Supplementary data to this article can be found online at https://doi.org/10.1016/j.rvsc.2021.08.014.

Declaration of Competing Interest

The authors have no competing interests to declare.

Acknowledgements

The study was supported by the KNOW (Leading National Research Centre) project of the Polish Ministry of Science and Higher Education

under funding decision no. 05-1/KNOW2/2015. We would like to thank Urszula Bocian for technical assistance. The authors are grateful to Prof. Marek Michalak (University of Alberta, Edmonton, AB, Canada) and Prof. Magdalena Dunowska (Massey University, Palmerston North, New Zealand) for critical comments.

References

Aldridge, G.M., Podrebarac, D.M., Greenough, W.T., Weiler, I.J., 2008. The use of total protein stains as loading controls: an alternative to high-abundance single-protein controls in semi-quantitative immunoblotting. J. Neurosci. Methods 172, 250–254. https://doi.org/10.1016/j.jneumeth.2008.05.003.

Alfano, C., Gladwyn-Ng, I., Couderc, T., Lecuit, M., Nguyen, L., 2019. The unfolded protein response: a key player in Zika virus-associated congenital microcephaly. Front. Cell. Neurosci. 13, 94. https://doi.org/10.3389/fncel.2019.00094.

Allen, G.P., Breathnach, C.C., 2006. Quantification by real-time PCR of the magnitude and duration of leucocyte-associated viraemia in horses infected with neuropathogenic vs. non-neuropathogenic strains of EHV-1. Equine Vet. J. 38, 252–257. https://doi.org/10.2746/042516406776866453.

Barodia, S.K., Prabhakaran, K., Karunakaran, S., Mishra, V., Tapias, V., 2019. Editorial: mitochondria and endoplasmic reticulum dysfunction in Parkinson's disease. Front. Neurosci. 13, 1171. https://doi.org/10.3389/fnins.2019.01171.

Bendtsen, J.D., Jensen, L.J., Blom, N., von Heijne, G., Brunak, S., 2004. Feature-based prediction of non-classical and leaderless protein secretion. Protein Eng. Des. Sel. 17, 349–356. https://doi.org/10.1093/protein/gzh037.

Bhattacharjee, G., Ahamed, J., Pedersen, B., El-Sheikh, A., Mackman, N., Ruf, W., Liu, C., Edgington, T.S., 2005. Regulation of tissue factor–mediated initiation of the coagulation cascade by cell surface grp78. Arterioscler. Thromb. Vasc. Biol. 25, 1737–1743. https://doi.org/10.1161/01.ATV.0000173419.31242.56.

Blackwood, E.A., Thuerauf, D.J., Stastna, M., Stephens, H., Sand, Z., Pentoney, A., Azizi, K., Jakobi, T., Van Eyk, J.E., Katus, H.A., Glembotski, C.C., Doroudgar, S., 2020. Proteomic analysis of the cardiac myocyte secretome reveals extracellular protective functions for the ER stress response. J. Mol. Cell. Cardiol. 143, 132–144. https://doi.org/10.1016/j.yjmcc.2020.04.012.

Boel, N.M.-E., Edkins, A.L., 2018. Regulation of the extracellular matrix by heat shock proteins and molecular chaperones. In: Binder, R.J., Srivastava, P.K. (Eds.), Heat Shock Proteins in the Immune System. Springer International Publishing, Cham, pp. 97–121. https://doi.org/10.1007/978-3-319-69042-1_6.

Burnett, H.F., Audas, T.E., Liang, G., Lu, R.R., 2012. Herpes simplex virus-1 disarms the unfolded protein response in the early stages of infection. Cell Stress Chaperones 17, 473–483. https://doi.org/10.1007/s12192-012-0324-8.

Chu, H., Chan, C.-M., Zhang, X., Wang, Y., Yuan, S., Zhou, J., Au-Yeung, R.K.-H., Sze, K.-H., Yang, D., Shuai, H., Hou, Y., Li, C., Zhao, X., Poon, V.K.-M., Leung, S.P., Yeung, M.-L., Yan, J., Lu, G., Jin, D.-Y., Gao, G.F., Chan, J.F.-W., Yuen, K.-Y., 2018. Middle East respiratory syndrome coronavirus and bat coronavirus HKU9 both can utilize GRP78 for attachment onto host cells. J. Biol. Chem. 293, 11709–11726. https://doi.org/10.1074/jbc.RA118.001897.

Edington, N., Bridges, C.G., Patel, J.R., 1986. Endothelial cell infection and thrombosis in paralysis caused by equid herpesvirus-1: equine stroke. Arch. Virol. 90, 111–124. https://doi.org/10.1007/BF01314149.

Gardai, S.J., McPhillips, K.A., Frasch, S.C., Janssen, W.J., Starefeldt, A., Murphy-Ullrich, J.E., Bratton, D.L., Oldenborg, P.-A., Michalak, M., Henson, P.M., 2005. Cell-surface calreticulin initiates clearance of viable or apoptotic cells through trans-activation of LRP on the phagocyte. Cell 123, 321–334. https://doi.org/10.1016/j.cell.2005.08.032.

Gardner, B.M., Pincus, D., Gotthardt, K., Gallagher, C.M., Walter, P., 2013. Endoplasmic reticulum stress sensing in the unfolded protein response. Cold Spring Harb. Perspect. Biol. 5, a013169. https://doi.org/10.1101/cshperspect.a013169.

Giorgi, C., Missiroli, S., Patergnani, S., Duszynski, J., Wieckowski, M.R., Pinton, P., 2015. Mitochondria-associated membranes: composition, molecular mechanisms, and Physiopathological implications. Antioxid. Redox Signal. 22, 995–1019. https://doi.org/10.1089/ars.2014.6223.

Goodman, L.B., Loregian, A., Perkins, G.A., Nugent, J., Buckles, E.L., Mercorelli, B., Kydd, J.H., Palù, G., Smith, K.C., Osterrieder, N., Davis-Poynter, N., 2007. A point mutation in a Herpesvirus polymerase determines Neuropathogenicity. PLoS Pathog. 3, e160 https://doi.org/10.1371/journal.ppat.0030160.

Greives, M.R., Samra, F., Pavlides, S.C., Blechman, K.M., Naylor, S.-M., Woodrell, C.D., Cadacio, C., Levine, J.P., Bancroft, T.A., Michalak, M., Warren, S.M., Gold, L.I., 2012. Exogenous calreticulin improves diabetic wound healing: Calreticulin improves diabetic wound healing. Wound Repair Regen. 20, 715–730. https://doi.org/10.1111/j.1524-475X.2012.00822.x.

Halperin, L., Jung, J., Michalak, M., 2014. The many functions of the endoplasmic reticulum chaperones and folding enzymes. IUBMB Life 66, 318–326. https://doi.org/10.1002/iub.1272.

Hensel, N., Raker, V., Förthmann, B., Buch, A., Sodeik, B., Pich, A., Claus, P., 2020. The proteome and Secretome of cortical brain cells infected with herpes simplex virus. Front. Neurol. 11, 844. https://doi.org/10.3389/fneur.2020.00844.

Holz, C.L., Nelli, R.K., Wilson, M.E., Zarski, L.M., Azab, W., Baumgardner, R., Osterrieder, N., Pease, A., Zhang, L., Hession, S., Goehring, L.S., Hussey, S.B., Soboll Hussey, G., 2017. Viral genes and cellular markers associated with neurological complications during herpesvirus infections. J. Gen. Virol. 98, 1439–1454. https://doi.org/10.1099/jgv.0.000773.

Holz, C.L., Sledge, D.G., Kiupel, M., Nelli, R.K., Goehring, L.S., Soboll Hussey, G., 2019. Histopathologic findings following experimental equine Herpesvirus 1 infection of horses. Front. Vet. Sci. 6, 59. https://doi.org/10.3389/fvets.2019.00059.

Honda, T., Horie, M., Daito, T., Ikuta, K., Tomonaga, K., 2009. Molecular chaperone BiP interacts with Borna disease virus glycoprotein at the cell surface. J. Virol. 83, 12622–12625. https://doi.org/10.1128/JVI.01201-09.

Ibrahim, I.M., Abdelmalek, D.H., Elshahat, M.E., Elfiky, A.A., 2020. COVID-19 spike-host cell receptor GRP78 binding site prediction. J. Inf. Secur. 80, 554–562. https://doi.org/10.1016/j.jinf.2020.02.026.

Jindadamrongwech, S., Thepparit, C., Smith, D.R., 2004. Identification of GRP 78 (BiP) as a liver cell expressed receptor element for dengue virus serotype 2. Arch. Virol. 149, 915–927. https://doi.org/10.1007/s00705-003-0263-x.

Jockheck-Clark, A.R., Bowers, E.V., Totonchy, M.B., Neubauer, J., Pizzo, S.V., Nicchitta, C.V., 2010. Re-examination of CD91 function in GRP94 (glycoprotein 96) surface binding, uptake, and peptide cross-presentation. J. Immunol. 185, 6819–6830. https://doi.org/10.4049/jimmunol.1000448.

Johnston, B.P., McCormick, C., 2019. Herpesviruses and the unfolded protein response. Viruses 12, 17. https://doi.org/10.3390/v12010017.

Kaufman, R.J., 2002. Orchestrating the unfolded protein response in health and disease. J. Clin. Invest. 110, 1389–1398. https://doi.org/10.1172/JCI16886.

Kelly, R., 1985. Pathways of protein secretion in eukaryotes. Science 230, 25–32. https://doi.org/10.1126/science.2994224.

Kydd, J.H., Lunn, D.P., Osterrieder, K., 2019. Report of the fourth international Havemeyer workshop on Equid Herpesviruses (EHV) EHV-1, EHV-2 and EHV-5. Equine Vet. J. 51, 565–568. https://doi.org/10.1111/evj.13141.

Laval, K., Poelaert, K.C.K., Van Cleemput, J., Zhao, J., Vandekerckhove, A.P., Gryspeerdt, A.C., Garré, B., van der Meulen, K., Baghi, H.B., Dubale, H.N., Zarak, I., Van Crombrugge, E., Nauwynck, H.J., 2021. The pathogenesis and immune evasive mechanisms of equine Herpesvirus type 1. Front. Microbiol. 12, 662686. https://doi.org/10.3389/fmicb.2021.662686.

Liu, B., Dai, J., Zheng, H., Stoilova, D., Sun, S., Li, Z., 2003. Cell surface expression of an endoplasmic reticulum resident heat shock protein gp96 triggers MyD88-dependent systemic autoimmune diseases. Proc. Natl. Acad. Sci. U. S. A. 100, 15824–15829. https://doi.org/10.1073/pnas.2635458100.

Malinowska, A., Kistowski, M., Bakun, M., Rubel, T., Tkaczyk, M., Mierzejewska, J., Dadlez, M., 2012. Diffprot — software for non-parametric statistical analysis of differential proteomics data. J. Proteome 75, 4062–4073. https://doi.org/10.1016/j.jprot.2012.05.030.

Medigeshi, G.R., Lancaster, A.M., Hirsch, A.J., Briese, T., Lipkin, W.I., DeFilippis, V., Fruh, K., Mason, P.W., Nikolich-Zugich, J., Nelson, J.A., 2007. West Nile virus infection activates the unfolded protein response, leading to CHOP induction and apoptosis. J. Virol. 81, 10849–10860. https://doi.org/10.1128/JVI.01151-07.

Meyer, B.A., Doroudgar, S., 2020. ER stress-induced secretion of proteins and their extracellular functions in the heart. Cells 9. https://doi.org/10.3390/cells9092066.

Michalak, M., Robert Parker, J.M., Opas, M., 2002. Ca2+ signaling and calcium binding chaperones of the endoplasmic reticulum. Cell Calcium 32, 269–278. https://doi.org/10.1016/s0143416002001884.

Moltedo, O., Remondelli, P., Amodio, G., 2019. The mitochondria-endoplasmic reticulum contacts and their critical role in aging and age-associated diseases. Front. Cell Dev. Biol. 7, 172. https://doi.org/10.3389/fcell.2019.00172.

Nain, M., Mukherjee, S., Karmakar, S.P., Paton, A.W., Paton, J.C., Abdin, M.Z., Basu, A., Kalia, M., Vrati, S., 2017. GRP78 is an important host factor for Japanese encephalitis virus entry and replication in mammalian cells. J. Virol. 91 https://doi.org/10.1128/JVI.02274-16.

Nugent, J., Birch-Machin, I., Smith, K.C., Mumford, J.A., Swann, Z., Newton, J.R., Bowden, R.J., Allen, G.P., Davis-Poynter, N., 2006. Analysis of Equid Herpesvirus 1 strain variation reveals a point mutation of the DNA polymerase strongly associated with Neuropathogenic versus Nonneuropathogenic disease outbreaks. J. Virol. 80, 4047–4060. https://doi.org/10.1128/JVI.80.8.4047-4060.2006.

Obeid, M., Tesniere, A., Ghiringhelli, F., Fimia, G.M., Apetoh, L., Perfettini, J.-L., Castedo, M., Mignot, G., Panaretakis, T., Casares, N., Métivier, D., Larochette, N., van Endert, P., Ciccosanti, F., Piacentini, M., Zitvogel, L., Kroemer, G., 2007. Calreticulin exposure dictates the immunogenicity of cancer cell death. Nat. Med. 13, 54–61. https://doi.org/10.1038/nm1523.

Oladunni, F.S., Horohov, D.W., Chambers, T.M., 2019. EHV-1: a constant threat to the horse industry. Front. Microbiol. 10, 2668. https://doi.org/10.3389/fmicb.2019.02668.

Ostrovsky, O., Ahmed, N.T., Argon, Y., 2009. The chaperone activity of GRP94 toward insulin-like growth factor II is necessary for the stress response to serum deprivation. Mol. Biol. Cell 20, 1855–1864. https://doi.org/10.1091/mbc.e08-04-0346.

Perez-Riverol, Y., Csordas, A., Bai, J., Bernal-Llinares, M., Hewapathirana, S., Kundu, D. J., Inuganti, A., Griss, J., Mayer, G., Eisenacher, M., Pérez, E., Uszkoreit, J., Pfeuffer, J., Sachsenberg, T., Yılmaz, Ş., Tiwary, S., Cox, J., Audain, E., Walzer, M., Jarnuczak, A.F., Ternent, T., Brazma, A., Vizcaíno, J.A., 2019. The PRIDE database and related tools and resources in 2019: improving support for quantification data. Nucleic Acids Res. 47, D442–D450. https://doi.org/10.1093/nar/gky1106.

Poelaert, K.C.K., Van Cleemput, J., Laval, K., Favoreel, H.W., Soboll Hussey, G., Maes, R. K., Nauwynck, H.J., 2018. Abortigenic but not neurotropic equine herpes virus 1 modulates the interferon antiviral defense. Front. Cell. Infect. Microbiol. 8, 312. https://doi.org/10.3389/fcimb.2018.00312.

Poelaert, K.C.K., Van Cleemput, J., Laval, K., Xie, J., Favoreel, H.W., Nauwynck, H.J., 2019. Equine herpesvirus 1 infection orchestrates the expression of chemokines in equine respiratory epithelial cells. J. Gen. Virol. 100, 1567–1579. https://doi.org/10.1099/jgv.0.001317.

Pronost, S., Léon, A., Legrand, L., Fortier, C., Miszczak, F., Freymuth, F., Fortier, G., 2010. Neuropathogenic and non-neuropathogenic variants of equine herpesvirus 1

in France. Vet. Microbiol. 145, 329–333. https://doi.org/10.1016/j.vetmic.2010.03.031.

Rozek, W., Kwasnik, M., Debski, J., Zmudzinski, J.F., 2013. Mass spectrometry identification of granins and other proteins secreted by neuroblastoma cells. Tumor Biol. 34, 1773–1781. https://doi.org/10.1007/s13277-013-0716-0.

Scheuner, D., Kaufman, R.J., 2008. The unfolded protein response: a pathway that links insulin demand with beta-cell failure and diabetes. Endocr. Rev. 29, 317–333. https://doi.org/10.1210/er.2007-0039.

da Silva, D.C., Valentão, P., Andrade, P.B., Pereira, D.M., 2020. Endoplasmic reticulum stress signaling in cancer and neurodegenerative disorders: tools and strategies to understand its complexity. Pharmacol. Res. 155, 104702. https://doi.org/10.1016/j.phrs.2020.104702.

Stasiak, K., Rola, J., Ploszay, G., Socha, W., Zmudzinski, J.F., 2015. Detection of the neuropathogenic variant of equine herpesvirus 1 associated with abortions in mares in Poland. BMC Vet. Res. 11, 102. https://doi.org/10.1186/s12917-015-0416-7.

Sutton, G., Thieulent, C., Fortier, C., Hue, E.S., Marcillaud-Pitel, C., Pléau, A., Deslis, A., Guitton, E., Paillot, R., Pronost, S., 2020. Identification of a new Equid Herpesvirus 1 DNA polymerase (ORF30) genotype with the isolation of a C2254/H752 strain in French horses showing no major impact on the strain behaviour. Viruses 12, 1160. https://doi.org/10.3390/v12101160.

Szklarczyk, D., Franceschini, A., Wyder, S., Forslund, K., Heller, D., Huerta-Cepas, J., Simonovic, M., Roth, A., Santos, A., Tsafou, K.P., Kuhn, M., Bork, P., Jensen, L.J., von Mering, C., 2015. STRING v10: protein–protein interaction networks, integrated over the tree of life. Nucleic Acids Res. 43, D447–D452. https://doi.org/10.1093/nar/gku1003.

Triantafilou, K., Fradelizi, D., Wilson, K., Triantafilou, M., 2002. GRP78, a coreceptor for coxsackievirus A9, interacts with major histocompatibility complex class I molecules which mediate virus internalization. J. Virol. 76, 633–643. https://doi.org/10.1128/jvi.76.2.633-643.2002.

Van Cleemput, J., Poelaert, K.C.K., Laval, K., Maes, R., Hussey, G.S., Van den Broeck, W., Nauwynck, H.J., 2017. Access to a main alphaherpesvirus receptor, located basolaterally in the respiratory epithelium, is masked by intercellular junctions. Sci. Rep. 7, 16656. https://doi.org/10.1038/s41598-017-16804-5.

Walter, P., Ron, D., 2011. The unfolded protein response: from stress pathway to homeostatic regulation. Science 334, 1081–1086. https://doi.org/10.1126/science.1209038.